JOURNAL OF SOLID STATE CHEMISTRY 19, 117–123 (1976)

A Mössbauer Study of the Relaxation Behavior of Dilute Fe^{3+} in $LiScO_2$ and Mullite

B. L. DICKSON* AND K. K. P. SRIVASTAVA

Department of Solid State Physics, Research School of Physical Sciences, Australian National University, Canberra, A.C.T. 2600, Australia

Received April 5, 1976

Mössbauer spectra of dilute Fe^{3+} in $LiScO_2$ and mullite have been studied over the temperature range 4 to 295°K. The hyperfine spectrum of the doublet $\pm\frac{1}{2}$ in mullite has been identified up to room temperature along with the spectrum of the doublet $\pm\frac{5}{2}$, which indicates that the spin–lattice relaxation times of doublets $\pm\frac{5}{2}$ and $\pm\frac{1}{2}$ are very similar in this system. The high value of the E/D ratio for tetrahedral Fe^{3+} in mullite has made possible the observation of well-resolved hyperfine spectra of the doublet $\pm\frac{1}{2}$ even in zero applied field.

Introduction

Small concentrations of Fe^{3+} ions in diamagnetic lattices often exhibit complex Mössbauer spectra at low temperatures as a result of slow electronic spin relaxation (*1*, *2*). In a noncubic crystal field, the $^6S_{5/2}$ ground state of Fe^{3+} splits into three Kramers doublets and, in the limit of long relaxation times, a contribution from each doublet, weighted by the appropriate Boltzmann factor, is seen in the Mössbauer spectrum. In an axial crystal field, the electronic spin–spin relaxation time is longest for the $\pm\frac{5}{2}$ doublet and shortest for the $\pm\frac{1}{2}$ one (*3*). The spin–lattice relaxation time for doublet $\pm\frac{5}{2}$ is also longer than for the doublet $\pm\frac{3}{2}$, but no such direct comparison is possible for the doublet $\pm\frac{1}{2}$ without a detailed knowledge of the phonon spectrum of the system (*4*, *5*). The spectrum from the $\pm\frac{1}{2}$ doublet is also sensitive to dipolar fields, as a result of coupling between nuclear and electronic spins associated with neighboring nuclei (*6*). For example, with Fe^{3+} in Al_2O_3 (*1*), the random nature of these dipolar fields results in the $\pm\frac{1}{2}$ doublet not being observed. Application of external fields of quite small magnitude (~ 100 Oe) can decouple the nuclear and electronic spins by producing an electronic Zeeman separation larger than the hyperfine energy and can allow the observation of the spectrum of the $\pm\frac{1}{2}$ doublet (*7*).

If the Fe^{3+} ion is placed in a crystal field with some rhombic distortion, the mixing between the Kramers doublets should both modify the relative relaxation rates of the doublets and decrease the effect of small applied fields. We have recently reported spectra of tetrahedral and octahedral Fe^{3+} ions doped into the $MgAl_2O_4$ spinel (*8*). The octahedral Fe^{3+} were in a site with a large rhombic distortion and contributions from the $\pm\frac{1}{2}$ doublet of these ions were distinguishable in the zero field spectra at 4.2°K. A large difference was also found in the relaxation rate of the two types of Fe^{3+}, which suggested a relation between the zero field splitting of the Kramers doublets and the type of spectrum observed at room temperature. In this paper we present analyzed spectra of Fe^{3+} in the diamagnetic lattices $LiScO_2$ and mullite

* Present address: C.S.I.R.O. Division of Mineral Physics, P.O. Box 136, North Ryde, New South Wales 2113, Australia.

Copyright © 1976 by Academic Press, Inc.
All rights of reproduction in any form reserved.
Printed in Great Britain

($3Al_2O_3 \cdot 2SiO_2$) to test the relation further and to obtain evidence on the effect of low symmetry crystal fields.

Experimental Methods

Preparation of Compounds. $LiScO_2$ was made by the powder reaction of Analar lithium carbonate and 99.9% scandium oxide at 1000°C.

Mullite was prepared in powder form by hydrolytically decomposing a stoichiometric mixture of aluminium and silicon alkoxides and heating the precipitate at 1550°C for 12 hr (*9*). X-ray powder patterns of the two materials showed them to be single phase within the limits of detection.

^{57}Fe was introduced into the three compounds by mixing the powders with ^{57}Fe-enriched ferric nitrate solution followed by careful evaporation to dryness. After heating slowly to around 700°C the powders were heated for 12 hr in air at 1250°C in the case of mullite and at 1100°C for $LiScO_2$. The powders were then ground and reheated several times to ensure uniform distribution of the Fe^{3+} ions.

Mössbauer spectra. The spectra were obtained with a constant acceleration spectrometer using a 30 mCi source of ^{57}Co in a palladium matrix. The velocity was calibrated against an iron foil absorber (*10*) and zero velocity was taken as the center of that spectrum.

Detailed Analysis

Hyperfine spectra may be analyzed in terms of a spin-Hamiltonian by comparing the experimental spectra to computer generated spectra (*1*); the appropriate spin-Hamiltonian for the interaction here is

$$H = H_{CF} + H_Q + g\mu_B \mathbf{H}\cdot\mathbf{S} + A\mathbf{I}\cdot\mathbf{S} - g_n\mu_n \mathbf{H}\cdot\mathbf{I}.$$

The last three terms are in the usual notation and describe the electronic Zeeman, nuclear hyperfine, and nuclear Zeeman interactions for the Fe^{3+} ion, respectively.

The quadrupole interaction H_Q in the $I = \frac{3}{2}$ excited nuclear state of ^{57}Fe is given by

$$H_Q = \frac{e^2qQ}{4I(2I-1)}\left[I_z^2 - \frac{I}{3}(I+1) + \frac{\eta}{2}(I_+^2 + I_-^2)\right],$$

so that the quadrupole splitting $\Delta E_Q = (P/2)(1 + (\eta^2/3)^{\frac{1}{2}}$ where $P = e^2qQ$. H_{CF} describes the interaction of the electronic spin with the crystal field surrounding the ion and is given by (*1*)

$$\begin{aligned} H_{CF} = {} & D[S_z^2 - \tfrac{1}{3}S(S+1)] + \frac{E}{2}(S_+^2 + S_-^2) \\ & + \frac{F}{180}[35S_z^4 - 30S(S+1)S_z^2 \\ & + 25S_z^2 - 6S(S+1) + 3S^2(S+1)^2] \\ & + \frac{a}{6}\left[S_\xi^4 + S_\zeta^4 + S_\mu^4 \right. \\ & \left. - \frac{S}{5}(S+1)(3S^2+3S-1)\right], \end{aligned}$$

where the (ξ,ζ,μ) axes lie along the cubic axes of the crystal field.

The Hamiltonian operates on the electron-nuclear base states $|SM_S\rangle|IM_I\rangle$. Diagonalization of the matrices for the ground and excited states yields the eigenlevels and eigenfunctions for both states. This was carried out by computer. Transition energies and probabilities were then calculated, and theoretical spectra for powdered samples were generated by repeating the calculation for many orientations of the magnetic field to the crystal axis. The method of Lang (*11*) was then used to obtain the full average spectrum.

In general, the analyses were made with A and g both assumed isotropic and g taking the value of 2.004. As the calculated spectra are insensitive to the asymmetry parameter, η, its value was taken as $3E/D$.

Results and Analysis

(a) Fe^{3+} in $LiScO_2$

Mössbauer spectra of the $LiScO_2$ doped with 0.1% Fe^{3+} were taken at 298, 77, and

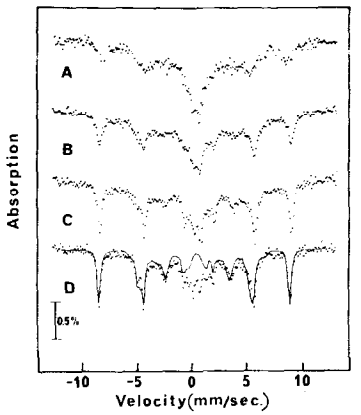

FIG. 1. Mössbauer spectra of ^{57}Fe-doped $LiScO_2$ at (A) 295°K, (B) 77°K, (C) 4.2°K, and (D) 4.2°K with an applied field of 185 Oe. The solid curve plotted over spectrum D was calculated with the parameters given in Table I and using a Lorentzian linewidth of 0.32 mm/sec.

4.2°K in zero field and at 4.2°K in a 185-Oe field, applied perpendicular to the γ-ray direction (Fig. 1). Cooling the sample slows the spin–lattice relaxation rate and sharp paramagnetic hyperfine structure is seen in the 4.2°K spectra. The effect of the applied field is small and leads to slight intensity changes. The doublet centered at 0.3 mm/sec with a splitting of 0.5 mm/sec in all the spectra is assigned to some pairs of Fe^{3+} ions having enhanced spin–spin relaxation rate. Attempts to remove this doublet by extended heating of the powder were not successful, but this does not affect the analysis of the data.

$LiScO_2$ has a tetragonal unit cell and the Fe^{3+} ions are expected to enter the Sc^{3+} site which has rhombic symmetry (*12*). Hence, the rhombic E term in H_{CF} slould be nonzero and the data were analyzed with E as a parameter and the crystal field axes (ξ,ζ,μ) taken to be coincident with the (x,y,z) axes. The best fitted curves for the 4.2°K spectra are shown in Fig. 1 and the derived parameters are listed in Table I.

The small value of $\lambda(=E/D)$ is consistent with the Fe^{3+} being in the Sc^{3+} site with a partly rhombic distortion of the site but contrasts with the previously reported high E/D value (*13*). The X-band (9.52 GHz) EPR spectrum of our sample of Fe^{3+}-doped $LiScO_2$ was obtained and showed a strong line at $g' = 4.75$, not $g' = 4.3$ as reported previously (*13*). Thus, the analysis of the 4.3 line as showing a large λ value is not valid. A further sharp line at $H \approx 500$ Oe indicates a zero field splitting between a pair of Kramers doublets of about 0.32 cm^{-1}. From the Mössbauer spectra the value of D was found to be in the range -0.16 to $-0.35\ cm^{-1}$. Hence, from the EPR spectrum D is obtained as $-0.16\ cm^{-1}$ with the low field line resulting from a $\pm\frac{3}{2}$ to $\pm\frac{1}{2}$ transition which has a splitting of $2D$.

(*b*) *Fe^{3+} in Mullite ($3Al_2O_3 \cdot 2SiO_2$)*

Mössbauer spectra of mullite doped with 0.09% $^{57}Fe^{3+}$ taken at 298, 77, and 4.2°K are

TABLE I

EXPERIMENTALLY DETERMINED PARAMETERS FOR Fe^{3+} IN $LiScO_2$ AND MULLITE

Parameter	$LiScO_2$	Mullite ($3Al_2O_3 \cdot 2SiO_2$)	
Site coordination number	6	~6	~4
Isomer shift	0.30	0.30	0.30 mm/sec
Quadrupole splitting	−0.42	0.90	0.70 mm/sec
Zero field splitting, D	−0.16	1.18	0.20 cm^{-1}
$\lambda = E/D$	0.03	0.051	0.23
$\mu = a/D$	−0.10	—	—
Ground state hyperfine coupling constant, A_g	−2.48	−2.64	−2.64 mm/sec
Associated hyperfine field, $\lvert H \rvert$	215	229 ± 2	229 ± 2 kOe/spin

shown in Fig. 2 and spectra taken in applied fields up to 300 Oe at 4.2 and 1.7°K are shown in Fig. 3. These spectra are more complex than

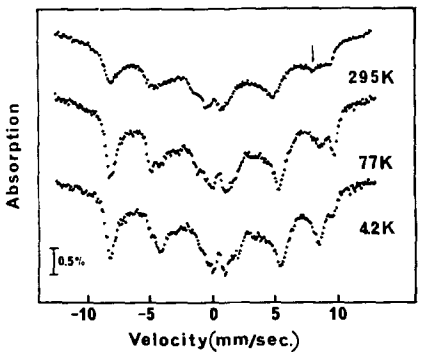

FIG. 2. Mössbauer data of ^{57}Fe-doped mullite at various temperatures in zero applied field. The arrow indicates the high velocity line assigned to the $\pm\frac{1}{2}$ Kramers doublet of tetrahedral Fe^{3+}.

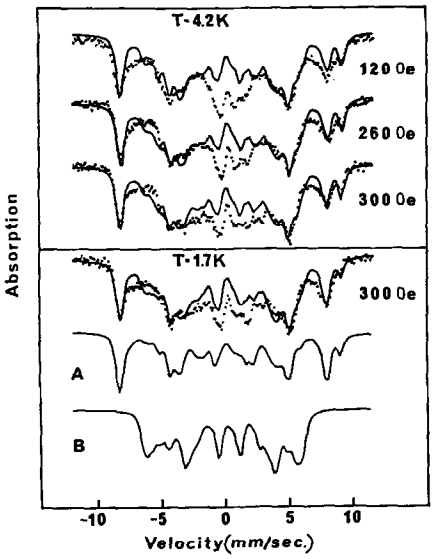

FIG. 3. Mössbauer spectra of mullite taken at 1.7 and 4.2°K in magnetic fields applied perpendicular to the γ-ray beam direction. The solid curves were calculated as described in the text with the parameters given in Table I and using a Lorentzian linewidth of 0.50 mm/sec. The calculated contributions from (A) the tetrahedral Fe^{3+} and (B) the octahedral Fe^{3+} to the spectrum of mullite taken at 1.7°K in a field of 300 Oe are shown individually.

those of Fe^{3+} in $LiScO_2$ and contain broadened lines. This is a result of the disorder in the unit cell of mullite, which contains 0.8 formula units (*14*). The consequent random distribution of lattice vacancies results in variations around the filled sites. In each unit cell, two Al atoms are octahedrally coordinated, with a mean Al–O bond length of 0.189 nm, 0.8 Al atoms are in a tetrahedral site of mean bond length 0.180 nm, and the remaining 2Al and 1.6Si are in a smaller tetrahedral site with the mean bond length varying between 0.172 and 0.175 nm. The structure can be considered to consist of chains of AlO_6 octahedra running parallel to the *c*-axis which are linked by groups of AlO_4 or SiO_4 tetrahedra.

As a result of this structural complexity, the Mössbauer spectra will be a summation over a wide range of different sites. To make analysis possible we have assumed that all the tetrahedral Fe^{3+} will give similar spectra and that the spectra can be treated as a sum of spectra of tetraheral ions and of octahedral ions. Initial values of D and E for Fe^{3+} in mullite were obtained from an EPR study of Fe^{3+} in natural sillimanite (*15*). The mullite structure is derived from the sillimanite structure (*16*) by removing some oxygen ions, randomizing the Al and Si ions and generating some new Al sites. The values of D and E for tetrahedral Fe^{3+} in sillimanite were found to be 0.174 and 0.054 cm^{-1}, respectively, whereas for the octahedral Fe^{3+} values of 1.18 and 0.138 cm^{-1} were obtained. The changes with temperature in the intensity of the two peaks near 8 mm/sec in the zero field spectra of mullite are consistent with Fe^{3+} ions of low D value giving these two lines, with a second type of Fe^{3+} ion having a large D value and giving a significant contribution to the central region. Thus the outer lines are assigned to tetrahedral Fe^{3+}.

The apparent large difference in D values for the two sites simplifies the fitting of the spectra. The parameters of the tetrahedral Fe^{3+} were first adjusted until the outer peaks in the spectra were well fitted. The spectrum of octahedral Fe^{3+} was then calculated and combined in various ratios with that of the tetrahedral Fe^{3+} until the broad peaks in the region of –4 mm/sec were well fitted. Because

of the lack of distinct outer peaks for the octahedral Fe^{3+}, the isomer shift and magnetic hyperfine constant, A, were initially taken equal to those of the tetrahedral ions but could not be refined further. The final parameters obtained are listed in Table I and the calculated spectra are shown in Fig. 3. A ratio of tetrahedral to octahedral Fe^{3+} of 1.7 was found to give the best result, a value slightly higher than the ratio of 1.4 of possible Al^{3+} sites in mullite.

The curves shown in Fig. 3 are poor fits to the data in the central region. The manner in which the peaks around 1 mm/sec broaden and spread out as a field is applied or the sample is cooled could indicate that there is a third type of ferric iron present. The room temperature spectrum of a sample with 0.18 at% Fe^{3+} showed a large contribution from the fast relaxing iron, resulting in a central quadrupole splitting. This is due to an iron ion with a close iron neighbor resulting in an enhanced spin–spin relaxation rate. With the 0.09% sample, similar iron pairs might be expected and could account for the deep absorption in the center of the 4.2°K spectra.

Despite the discrepancies between the calculated curve and the data, the two parameters D and E can be obtained with some confidence, and there is good agreement of the crystal field parameters of Fe^{3+} in mullite and sillimanite. It is interesting to note that octahedrally coordinated Fe^{3+} ions in the other two Al_2SiO_5 polymorphs, kyanite and andalusite, also have large D values of 1.3 (*17*) and 1.88 cm^{-1} (*18*), respectively.

Discussion

The results presented here illustrate a number of features of paramagnetic hyperfine spectra of dilute Fe^{3+}. In the case of $LiScO_2$ the need for care in analyzing lines near $g = 4.3$ in EPR spectra is clearly seen, and as recently shown (*19*), a line at this position can arise for any value of λ provided the relation $4\mu = 3(1-3\lambda)$ holds, where $\mu = a/D$. With mullite, an example is obtained of the effect that with a high value of λ the spectrum from a $\pm\frac{1}{2}$ Kramers doublet becomes observable in zero applied field. Calculated spectra of the $\pm\frac{1}{2}$ doublet for the tetrahedral Fe^{3+} in mullite (Fig. 4) show that above an internal field of 5 Oe the line at 8.2 mm/sec is almost field independent. This is the line which is also observed at 295°K, indicating that the spin–lattice relaxation times of the doublets $\pm\frac{5}{2}$ and $\pm\frac{1}{2}$, or of all the three doublets, are very similar, if the spin–spin relaxation is ignored in very dilute systems. It is difficult to say whether the similar spin–lattice relaxation times for the doublets $\pm\frac{5}{2}$ and $\pm\frac{1}{2}$ is a unique feature of this system only or is generally true, because in other systems studied so far the spectra from the doublet $\pm\frac{1}{2}$ has not been so clearly identifiable at high temperatures.

The hyperfine spectra from paramagnetic Fe^{3+} have been studied in various diamagnetic lattices over a wide range of temperatures, and these results throw some light on the spin–lattice relaxation process of Fe^{3+}. The tetrahedral Fe^{3+} in $LiAl_5O_8$ ($D = -0.101$ cm^{-1}) (*20*), $MgAl_2O_4$ ($D = -0.08$ cm^{-1}) (*8*), and mullite ($D = 0.20$ cm^{-1}), and octahedral Fe^{3+} in Al_2O_3 ($D = 0.176$ cm^{-1}) (*1, 2, 21*), $LiScO_2$ ($D = -0.16$ cm^{-1}), and alum ($D = 0.024$ cm^{-1}) (*22*) all show almost no temperature dependence of relaxation time between 4.2 and 77°K. This indicates a spin–lattice relaxation time of $>10^{-7}$ sec in this temperature range. Thus both the tetrahedral and octrahedral Fe^{3+} show similar relaxation behavior for values of $|D|$ less than 0.20 cm^{-1}. At 295°K the spectra for all these different

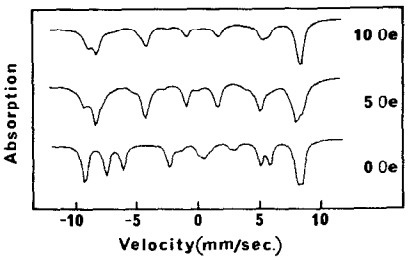

FIG. 4. Computed spectra of the $\pm\frac{1}{2}$ Kramers doublet of tetrahedral Fe^{3+} in mullite with the presence of internal random fields of 0, 5, and 10 Oe and no applied field. The model of Viccaro *et al.* (*20*) for approximating the effects of the magnetic moments of the neighboring nuclei as a static random magnetic field was used in the calculation.

systems, except alum, show well-resolved paramagnetic hyperfine structure. However, the line broadening between spectra taken at 77 and 295°K is almost negligible in the spectra of $LiAl_5O_8$, small in the case of $MgAl_2O_4$, larger with Al_2O_3 and mullite, and very marked with $LiScO_2$. Details of the temperature-dependence of spin–lattice relaxation times require the change in linewidth to be measured over a temperature range. This has been done for the case of Fe^{3+} in Al_2O_3 (*21*) where the spin–lattice relaxation time, τ_{SL}, was found to be proportional to T^{-2} for temperatures above 90°K. A relaxation time proportional to $T^{-1.5}$ is estimated for Fe^{3+} in mullite and $LiScO_2$ by comparison of the 295°K spectra with calculated spectra of Fe^{3+} with varying relaxation time (*23*). This indicates a similarity of relaxation times for Fe^{3+} in Al_2O_3, mullite, and $LiScO_2$. For Fe^{3+} in spinel and $LiAl_5O_8$ the relaxation time is still less temperature dependent between 77 and 295°K.

The relaxation behavior of the octahedral Fe^{3+} in mullite ($D = 1.18$ cm^{-1}) could not be determined as no separate peak for these ions is identifiable in the 77 or 295°K spectra. However, the lack of any strong central peak at 295°K does indicate that the relaxation rate is not fast. The mullite spectrum at 295°K appears to sit on a broad, featureless absorption which is probably due to octahedral Fe^{3+} with a wide range of intermediate relaxation rates. This behavior is very similar to that observed for octahedral Fe^{3+} ($D = 0.50$ cm^{-1}) in $MgAl_2O_4$ (*8*) which also has a large D value. The octahedral Fe^{3+} in $MgAl_2O_4$ gives a sharp contribution at 77°K, but only a very broad absorption at 295°K due to an enhanced spin–lattice relaxation rate at higher temperature. However, again this relaxation rate is not fast enough to produce a central peak. The hyperfine spectrum of Fe^{3+} in TiO_2 ($D = 0.68$ cm^{-1}) (*24*) also remains observable, though broadened, from 4.2 to 295°K. These observations indicate that for Fe^{3+} with D values between 0.50 and 1.18 cm^{-1} the temperature dependence of spin–lattice relaxation time may not differ from those with $|D| \leqslant 0.20$ cm^{-1}.

These results may be compared with the expression obtained by Svetozarov (*5*) in studying the relative importance of single-phonon and two-phonon spin–lattice relaxation processes between Kramers doublets of an S-state ion. In terms of the crystal field splitting $\Delta(\simeq 6D)$, Debye temperature θ_D and velocity of sound c, in the lattice, the single-phonon relaxation time, τ_{SL}^S, is given by

$$\tau_{SL}^S \sim mc^2\theta_D{}^3\,\Delta^{-5},\ T \ll \Delta \quad \text{or}$$
$$\sim mc^2\theta_D{}^3\Delta^{-4}T^{-1},\quad T \gg \Delta,$$

and the direct two-phonon relaxation time, τ_{SL}^D, as

$$\tau_{SL}^D \sim 10^{-5}(mc^2)^2\theta_D{}^6\,\Delta^{-2}T^{-7},\ T \ll \theta_D \quad \text{or}$$
$$\sim 10^{-3}(mc^2)^2\theta_D\Delta^{-2}T^{-2},\ T \gg \theta_D.$$

These expressions show that for small crystal field splittings the single-phonon processes dominate, but with increase in temperature the direct two-phonon processes become more important at a certain temperature. The probability of an indirect two phonon (or Raman) process for small crystal field splittings is small compared with that of the direct two phonon process and may be neglected (*5*).

Though these expressions are valid in limiting cases only, the observed temperature dependence of spin–lattice relaxation time for Fe^{3+} in the above-mentioned systems roughly follows the pattern predicted by the high temperature ($T \gg \Delta$) single-phonon process or the direct two-phonon process for $T \gg \theta_D$. However, it is very unlikely that the temperature range of 77 to 295°K is much greater than the Debye temperatures of Fe^{3+} in these systems. Hence the two-phonon process for $T \gg \theta_D$ may not be applicable, but if the high temperature ($T \gg \Delta$) single-phonon process is used to account for changes in relaxation times certain discrepancies become apparent. The D values of tetrahedral Fe^{3+} in mullite and spinel differ by a factor of 2.5. We do not observe the order of magnitude difference in the relaxation times predicted by the single-phonon process. Similarly, the relaxation behaviors of Fe^{3+} in Al_2O_3, mullite, and $LiScO_2$ are somewhat different in the temperature range 77 to 295°K, though

they all have similar small $|D|$ values. These minor discrepancies may be attributed to somewhat different Debye temperatures and velocities of acoustic phonons in these systems.

Similarly for Fe^{3+} in complex organic molecules like ferrichrome A ($D = 0.53$ cm^{-1}) (*23*, *25*) and zerolite (*4*), the τ_{SL} appears to vary as $T^{-1.5}$ to T^{-2} over about 20 to 150°K, though the absolute relaxation times are smaller (than for Al_2O_3, mullite, or spinel), so that the linebroadening due to relaxation effects can be observed at much lower temperatures (< 10°K for ferrichrome A, and < 27°K for zerolite). This relatively smaller absolute relaxation time in organic molecules may possibly be due to smaller Debye temperatures and/or a smaller velocity of sound. Similar reasons may be responsible for the somewhat different relaxation behavior of Fe^{3+} in the complex alum (*22*) molecules, compared to that in spinel and alumina.

From these observations it is clear that for Fe^{3+} the two-phonon spin–lattice relaxation process represented by $\tau_{SL} \alpha T^{-7}$ remains quite negligible. This may be the characteristic of the S-state Fe^{3+} ion which is weakly coupled to the lattice.

Acknowledgment

The authors would like to thank W. T. Oosterhuis for the use of his computer program, and Dr. R. Bramley of the Research School of Chemistry, Australian National University, for taking EPR spectra of $LiScO_2:Fe^{3+}$.

References

1. H. H. WICKMAN AND G. K. WERTHEIM, *Phys. Rev.* **148**, 211 (1966).
2. G. K. WERTHIUM AND J. P. REMEIKA, *in* "Proceedings of the XIII Colloque Ampére, Louvain, Belgium, 1964," p. 147, North-Holland, Amsterdam (1965)
3. M. BLUME, *Phys. Rev. Letters*, **14**, 96 (1965); **18**, 305 (1967).
4. I. P. SUZDALEV, A. M. AFANAS'EV, A. S. PLACHINDA, V. I. GOL'DANSKII, AND E. F. MAKAROV, *Sov. Phys. JETP* **28**, 923 (1969).
5. V. V. SVETOZAROV, *Sov. Phys. Solid State* **12**, 826 (1970).
6. A. M. AFANAS'EV AND YU M. KAGAN, *JETP Lett.* **8**, 382 (1968).
7. V. D. GOROBCHENKO, I. I. LUKASHEVICH, V. V. SKLYAREVSKII, K. F. TSITSKISHUILLI, AND N. I. FILIPPOV, *JETP Lett.* **8**, 386 (1968).
8. B. L. DICKSON AND K. K. P. SRIVASTAVA, *J. Phys. Chem. Solids*, **37**, 447 (1976).
9. K. S. MAZDIYASNI AND L. M. BROWN, *J. Amer. Ceram. Soc.* **55**, 548 (1972).
10. C. E. VIOLET AND D. N. PIPKORN, *J. Appl. Phys.* **42**, 4339 (1971).
11. G. LANG, *J. Chem. Soc.* (*A*) 3608 (1971).
12. R. HOPPE, B. SCHEPORS, H. RÖHRBORN, AND E. VIELHABER, *Z. Anorg. Allgem. Chem.* **339**, 130 (1965).
13. T. BIRCHALL AND A. F. REID, *J. Solid State Chem.* **6**, 411 (1973).
14. C. W. BURNHAM, *Carnegie Inst. Washington Year Book* **63**, 223 (1963–1964).
15. J. LE MARSHALL, D. R. HUTTON, G. J. TROUP, AND J. R. W. THYER, *Phys. Status Solidi* **A5**, 769 (1971).
16. C. W. BURNHAM, *Carnegie Inst. Washington Year Book* **62**, 158 (1962–1963).
17. G. J. TROUP AND D. R. HUTTON, *Brit. J. Appl. Phys.* **15**, 1493 (1964).
18. F. HOLUJ, J. R. THYER, AND N. E. HEDGECOCK, *Canad. J. Phys.* **44**, 509 (1966).
19. K. SPARTALIAN, W. T. OOSTERHUIS, AND J. B. NEILANDS, *J. Chem. Phys.* **62**, 3538 (1975).
20. P. J. VICCARO, F. DE S. BARROS, AND W. T. OOSTERHUIS, *Phys. Rev.* **B5**, 4257 (1972).
21. V. P. KORNEEV, I. P. SUZLADEV, V. I. GOL'DANSKII, T. YA. KURENEVA, E. F. MAKAROV, AND A. S. PLACHINDA, *Sov. Phys. Solid State* **13**, 291 (1971).
22. L. E. CAMPBELL AND S. DE BENEDETTI, *Phys. Rev.* **167**, 345 (1966).
23. H. H. WICKMAN, M. P. KLEIN, AND D. A. SHIRLEY, *Phys. Rev.* **152**, 345 (1966).
24. M. ALAM, S. CHANDRA, AND G. R. HOY, *Phys. Letters* **22**, 26 (1966).
25. W. T. OOSTERHUIS AND K. SPARTALIAN, *J. Physique, Coll. 35* **C6**, 347 (1974).